Proc. SPIE, Vol.8440 (2012) 84400Q-1 ~ 84400Q-10 [10 pages]

Magic-wavelength optical dipole trap of cesium and rubidium atoms

Junmin Wang*, Yongjie Cheng, Shanlong Guo, Baodong Yang, Jun He
State Key Laboratory of Quantum Optics and Quantum Optics Devices of China (Shanxi University), and Institute of Opto-Electronics, Shanxi University,
92 Wu Cheng Road, Taiyuan 030006, Shanxi Province, P. R. China

ABSTRACT

Optical dipole traps (ODT) with far-off-resonance laser are important tools in more and more present cold-atom experiments, which allow confinement of laser-cooled atoms with a long storage time. Particularly, the magic wavelength ODT can cancel the position-dependent spatially inhomogeneous light shift of desired atomic transition, which is introduced by the ODT laser beam. Now it plays an important role in the state-insensitive quantum engineering and the atomic optical clock. To verify the magic wavelength or the magic wavelength combination for D_2 line transition of cesium (Cs) and rubidium (Rb) atoms, we calculated and analyzed the light shift of the ^{133}Cs $6S_{1/2}$ - $6P_{3/2}$ transition for a monochromatic ODT, and also the ^{87}Rb $5S_{1/2}$ - $5P_{3/2}$ transition for a dichromatic ODT with a laser frequency ratio of 2:1. Also a dichromatic magic-wavelength ODT laser system for ^{87}Rb atoms is proposed and experimentally realized by employing the quasi-phase-matched frequency doubling technique with telecom laser and fiber amplifier.

Keywords: optical dipole trap, dichromatic optical dipole trap, magic wavelength, light shift, cesium atoms, rubidium atoms

1. INTRODUCTION

Optical dipole traps (ODT) with a far-off-resonance laser become a basic tool in more and more present cold-atom experiments and allow confinement of laser-cooled neutral atoms for a long storage time but with a very low photon scattering rate [1-3]. The essence of ODT is the position-dependent spatially inhomogeneous light shift of atomic ground state coming from the interaction between the light-induced dipole moment of the neutral atoms and the trapping laser field with a gradient intensity profile.

ODT now is frequently utilized for trapping cold atoms which are prepared in well-defined quantum state for both internal and external degrees of freedom. To realize the atomic initial state preparation and atomic internal state coherent manipulation people need to calculate the exact light shift of ground state (connected with trap depth of ODT) and excited state for accurate adjustment of laser's detuning related to atoms confined in ODT. If the desired atomic transition frequency of atoms in ODT can be kept the same as in the case of free space with zero field [4-7], in the other words, ODT only traps atoms at certain spatial position but it does not perturb the specific transition frequency, it will be very helpful for much more precisely measuring desired atomic transition or stabilizing laser's frequency to desired ultra-narrow atomic transition as well as coherently controlling atomic internal state but independent of the atomic residual thermal motion. Actually to make light shift of the ground state and the upper state equal, people can tailor the light shift of atomic state by using trapping laser with a proper wavelength, which is the so-called magic wavelength [4-7]. Since the concept of magic wavelength was considered firstly by Katori group for strontium (Sr) atoms [4], later by Kimble group [5] and Cho group [6] for cesium (Cs) atoms, now it plays an important role in the state-insensitive quantum engineering and the Sr and ytterbium (Yb) atomic optical clock [8].

To verify the magic wavelength or the magic wavelength combination for D_2 line transition of ^{133}Cs and rubidium-87 (^{87}Rb) atoms, we calculated and analyzed the light shift of the ^{133}Cs $6S_{1/2}$ $|F=4\rangle$ - $6P_{3/2}$ $|F'=5\rangle$ transition for a monochromatic ODT, and also the ^{87}Rb $5S_{1/2}$ $|F=2\rangle$ - $5P_{3/2}$ $|F'=3\rangle$ transition for a dichromatic ODT with a laser frequency ratio of 2:1. Especially the dichromatic ODT with magic wavelength combination actually expands the magic wavelength concept, and we hope it may find more applications to coherently control the atomic internal state independent of the atomic residual thermal motion. We aim at employing magic wavelength microscopic ODT to confine single atom (single ^{133}Cs atom [9, 10] or single ^{87}Rb atom [11]) to explore triggered single-photon source based on

---

* **Corresponding author, wwjjmm@sxu.edu.cn; Phone: +86-351-7011844; Fax: +86-351-7011500**

Quantum Optics II, edited by Thomas Durt, Victor N. Zadkov, Proc. of SPIE Vol. 8440, 84400Q · © 2012 SPIE · CCC code: 0277-786X/12/$18 · doi: 10.1117/12.922113

fluorescence radiation from a two-level single emitter (here single atom) with the periodical coherent excitations [11], and magic wavelength ODT will improve the efficiency of coherent excitation of atom to the upper state as well as the distinguishability degree of single photons.

Also a dichromatic magic-wavelength laser system for a ODT of ^{87}Rb atoms was proposed and experimentally realized by employing the quasi-phase-matched (QPM) efficient laser frequency doubling technique with telecom laser and fiber amplifier.

2. CALCULATION METHOD OF LIGHT SHIFT

Usually calculation of light shift, especially for atomic ground state, can be approximately simplified into a two-level model from the classical oscillator model, in which the ODT potential for atoms can be expressed as follows [3] :

$$U_{dip}(r) = \frac{3\pi c^2}{2\omega_0^3} \cdot \frac{\Gamma}{\omega - \omega_0} \cdot I(r) \tag{1}$$

here ω_0 is the angular transition frequency between atomic ground state and excited state, ω is the angular frequency of light field, Γ is the spontaneous decay rate, and I(r) is the distribution of light intensity. Main physical feature of ODT is clear according to this simple two-level model. When the detuning $(\omega - \omega_0) < 0$ (red detuning), ODT potential for atomic ground state (U_{dip}) is negative, and it attracts atoms to the point with maximum intensity. In contrast, when the detuning $(\omega - \omega_0) > 0$ (blue detuning), U_{dip} is positive, and it repulses atoms to the point with minimum intensity.

But actually this simple two-level model is not so accurate for calculation of light shift of ground state and especially for excited state, because of the multi-levels of real atoms. Taking Cs atoms as an example, we calculate the light shift of cesium atoms in an ODT formed by focusing TEM_{00}-mode 1064-nm laser, considering |a> state (one hyperfine fold of Cs $6S_{1/2}$ state), |b> state (one hyperfine fold of Cs $6P_{3/2}$ state) and |c> state (one hyperfine fold of Cs $8S_{1/2}$ state, for example), as shown in Figure 1. The 1064-nm ODT laser is far red-detuned from |a> - |b> transition (852 nm) and |b> - |c> transition (794 nm). According to the two-level model, if we do not consider |c> state, the light shift of |a> state is negative while that of |b> state is positive (as shown in the left column in Figure 1). If we do not consider |a> state, the light shift of |b> state is negative while that of |c> state is positive (as shown in the middle column in Figure 1). So one question should be raised, what is the actual sign of light shift of |b> state (negative or positive, even not perturbed, see the right column in Figure 1)? To address this question, one have to carefully analyze and calculate the light shift by using of the multi-level model in which many dipole-allowed transitions connected to |b> state should be included. In fact, to calculate the light shift of any atomic state more precisely, many dipole-allowed transitions connected to this state should be considered (the multi-level model), instead of the simplified two-level model. If light shift of |b> state equals to that of |a> state, then the wavelength of ODT laser is the above-mentioned magic wavelength for |a> - |b> transition, with which the |a> - |b> transition frequency will be kept the same as in the case of zero field. As discussed in the introduction the magic-wavelength ODT plays a more and more important role in precise measurement and quantum engineering with cold atoms due to its "magic" feature.

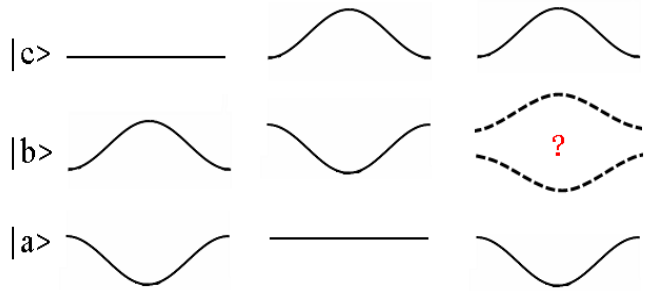

Figure 1. Schematic diagram of the light shift of multi-level atom based on the simple two-level model. The ODT laser is red detuned to |a> - |b> and |b> - |c> transitions. Based on the two-level model only |a> and |b> states are considered in the left column, and only |b> and |c> states are considered in the middle column. To more precisely calculate the light shift of each state (especially state |b>) the multi-level model is needed, in which one should include many dipole-allowed transitions connected with the desired state.

According to the second-order perturbation theory, the light shift U_{dip} of atomic state in ODT laser field can be expressed as follows: [3]

$$U_{dip} = -\frac{1}{2}\left\langle \vec{P}\cdot\vec{E} \right\rangle = -\frac{1}{2\varepsilon_0 c}\mathrm{Re}(\alpha) I(r) \tag{2}$$

here $\vec{P}$ is the induced dipole moment, $\vec{E}$ is the electric filed of the ODT laser, α is the polarizability of the atomic state, and I(r) is the distribution of light intensity. It is straightforward to calculate the polarizability α by integration of the equation of motion $\ddot{x} + \Gamma_\omega \dot{x} + \omega_0^2 x = -eE(t)/m_e$ in Lorentz's model of a classical oscillator. Here $\Gamma_\omega = e^2\omega^2/6\pi\varepsilon_0 m_e c^3$ is the classical damping rate due to the radiative loss. Substituting $e^2/m_e = 6\pi\varepsilon_0 c^3\Gamma_\omega/\omega^2$ and introducing the on-resonance damping rate $\Gamma \equiv \Gamma\omega_0 = \Gamma_\omega(\omega_0/\omega)^2$, the polarizability can be expressed as follows:

$$\alpha = 6\pi\varepsilon_0 c^3 \frac{\Gamma/\omega_0^2}{\omega_0^2 - \omega^2 - i\left(\omega^3/\omega_0^2\right)\Gamma} \tag{3}$$

$$\Gamma = \frac{\omega_0^3}{3\pi\varepsilon_0\hbar c^3}\left|\langle IJ'F'm'|D|IJFm\rangle\right|^2 \tag{4}$$

here I is the nuclear spin, J is the angular momentum, F is the total angular momentum of atomic state, m is the magnetic quantum number of atomic Zeeman state, D is the dipole operator, $\langle IJ'F'm'|D|IJFm\rangle$ is the dipole matrix element.

The real part of the polatizability of desired atomic state, Re(α), can be calculated by summing up the contributions from as many dipole-allowed transitions connected with this state as possible [3]:

$$\mathrm{Re}(\alpha) = \sum_{J'F'm'} 6\pi\varepsilon_0 c^3 \frac{1}{\omega_0^2\left(\omega_0^2 - \omega^2\right)} \frac{\omega_0^3}{3\pi\varepsilon_0\hbar c^3}\left|\langle IJ'F'm'|D|IJFm\rangle\right|^2 \tag{5}$$

The next task is the reduction of the dipole matrix element.

$$\left|\langle IJ'F'm'|\mu|IJFm\rangle\right|^2 = (2F+1)\left|\left(J'\|D\|J\right)\right|^2 \times \left\{\begin{matrix} J & J' & 1 \\ F' & F & I \end{matrix}\right\}^2 \left|c_{F,m}^{F',m'}\right|^2 \tag{6}$$

here the quantity in curly brackets is the Wigner 6-j symbol, the shorthand notation $c_{F,m}^{F',m'}$ for the Clebsch-Gordan coefficients is explicitly given as follows:

$$c_{F,m}^{F',m'} = \langle Fm|p|F'm'\rangle = (-1)^{m+F-1}\sqrt{2F'+1}\begin{pmatrix} F & 1 & F' \\ m & p & -m' \end{pmatrix} \tag{7}$$

here the quantity in round brackets is the Wigner 3-j symbol, and p = 0, ±1 stands for π and $\sigma^{\pm}$ transitions between the related states (the selection rule is m' = m + p). We choose the following normalization for the reduced matrix element, expressed in terms of the Einstein coefficients $A_{J'\to J}$ of state J' in the case of one decay channel J'→J:

$$\left|\left(J'\|D\|J\right)\right|^2 = A_{J'\to J}(2J'+1)\frac{3\pi\varepsilon_0\hbar c^3}{\omega_{JJ'}^3} \tag{8}$$

3. LIGHT SHIFT OF CESIUM-133 $6S_{1/2}$ AND $6P_{3/2}$ STATES

We calculated the light shift of ^{133}Cs $6S_{1/2}$ and $6P_{3/2}$ states. Figure 2 shows the light shift of all hyperfine folds and related all Zeeman sublevels of $6S_{1/2}$ and $6P_{3/2}$ states of ^{133}Cs atoms in an ODT formed by a strongly-focused linearly-polarized Gaussian laser beam with power of 30 mW and a waist radius of 2.3 μm (here these values are typical numbers in our

ODT experiment [9, 10], corresponding to intensity of I_0=3.6×10^5 W/cm^2), while the ODT laser wavelength changes from 600 nm to 1100 nm.

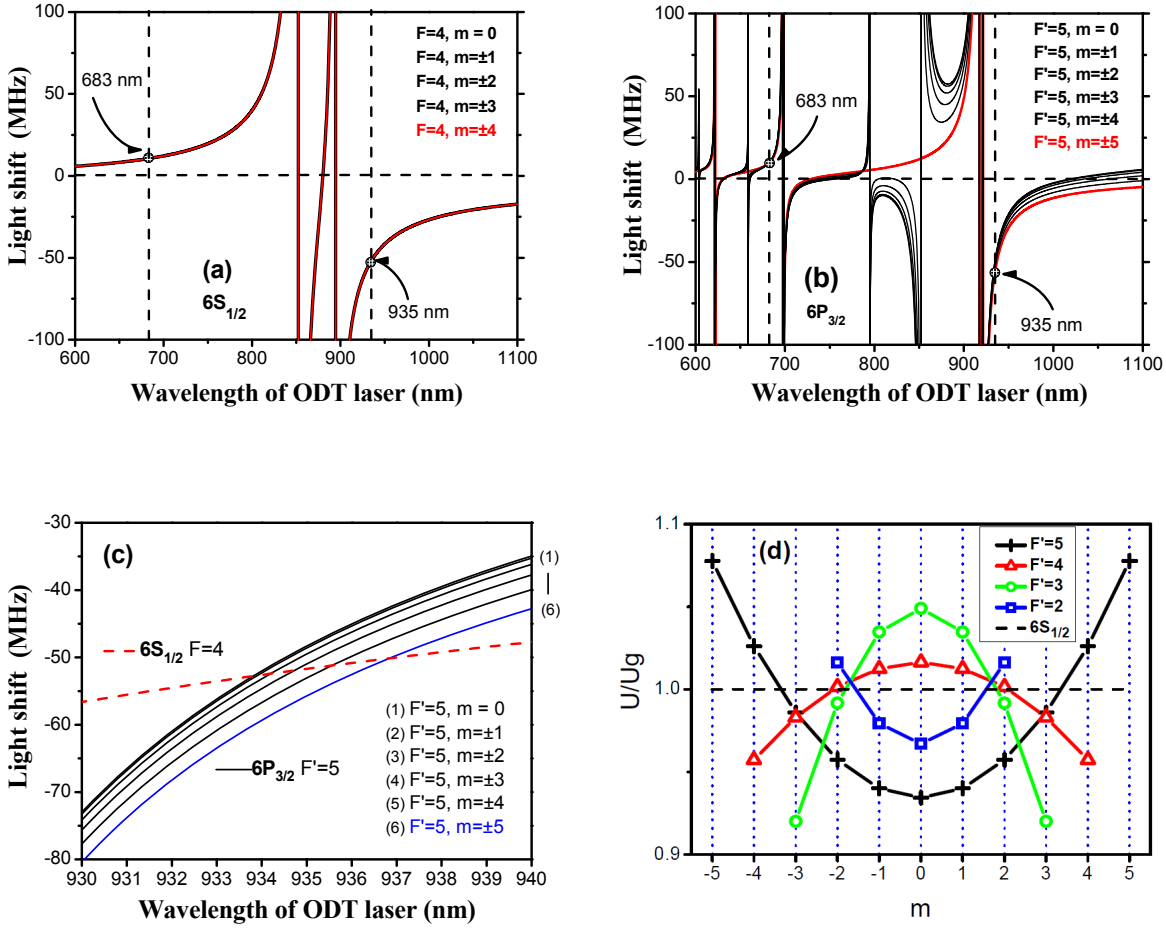

Figure 2. (Color online) Calculation results of the light shift of ^{133}Cs 6S$_{1/2}$ F = 4 state **(a)** and 6P$_{3/2}$ F' = 5 state **(b)** versus the wavelength of ODT laser. ODT is formed by a linearly-polarized strongly-focused TEM$_{00}$-mode Gaussian laser beam with intensity of I_0 = 3.6×10^5 W/cm^2. The two vertical dashed lines in **(a)** and **(b)** indicate magic wavelength of ~ 935nm at the red-detuning side and ~ 683nm at the blue-detuning side respectively. **(c)** shows the red-detuned magic wavelengths around ~ 935nm for 6S$_{1/2}$ F = 4 - 6P$_{3/2}$ F' = 5 transition included all Zeeman sublevels. **(d)** shows light shift of Zeeman sublevels for each 6P$_{3/2}$ excited hyperfine fold in the case of ~ 935 nm (magic wavelength) ODT laser with intensity of I_0 = 3.6×10^5 W/cm^2.The scaling in **(d)** is relative to light shift of 6S$_{1/2}$ ground state (Ug). The connection lines between data points in **(d)** are just for guiding eyes.

Our calculations included *n*P states up to 10P for ^{133}Cs 6S$_{1/2}$ state, and *n*S states up to 10S and *n*D states up to 10D for ^{133}Cs 6P$_{3/2}$ state. The Einstein *A* coefficients and vacuum wavelengths for the dipole-allowed transitions we considered here come from atomic line data on website (see **[12]**). The line which represents the light shift of all Zeeman sublevels of ^{133}Cs 6S$_{1/2}$ F = 4 state in Figure 2(a), 2(c) and 2(d) is degenerate for P=0 (a linearly-polarized ODT laser), however the light shifts of all Zeeman sublevels of ^{133}Cs 6P$_{3/2}$ F'=5 state split, as shown in Figure 2(b), 2(c) and 2(d). It is expected by equation (1) or (5) that the Dipole-allowed transition lines correspond to singular points. In Figure 2(a) two singular points for 6S$_{1/2}$ F = 4 state are indicated: 852.3 nm for the 6S$_{1/2}$ - 6P$_{3/2}$ transition (D$_2$ line), and 894.6 nm for the 6S$_{1/2}$ - 6P$_{1/2}$ transition (D$_1$ line). In Figure 2(b) ten singular points for 6P$_{3/2}$ F'=5 state are indicated: 603.6 nm for 6P$_{3/2}$ - 10S$_{1/2}$ transition, 658.8 nm for 6P$_{3/2}$ - 9S$_{1/2}$ transition, 794.6 nm for 6P$_{3/2}$ - 8S$_{1/2}$ transition, 852.3 nm for 6P$_{3/2}$ - 6S$_{1/2}$ transition, 621.93 nm and 621.48 nm for 6P$_{3/2}$ - 8D$_{3/2}$ and 6P$_{3/2}$ - 8D$_{5/2}$ transitions (too close to distinguish), 698.54 nm

and 697.52 nm for $6P_{3/2}$ - $7D_{3/2}$ and $6P_{3/2}$ - $7D_{5/2}$ transitions (too close to distinguish), 921.47 nm and 917.47 nm for $6P_{3/2}$ - $6D_{3/2}$ and $6P_{3/2}$ - $6D_{5/2}$ transitions (too close to distinguish). The two vertical dashed lines in Figure 2(a) and 2(b) indicate magic wavelength of ~ 935 nm at the red detuning side and ~ 683 nm at the blue detuning side respectively. Especially the magic wavelength of ~ 683nm at the blue-detuning side is much more interesting, because it allows to implement the optical bottle-beam ODT with this blue-detuning magic wavelength to trap ^{133}Cs atoms inside the optical "bottle" (the laser intensity is close to zero) with much lower photon scattering rate than the normally used red-detuning ODT. Figure 2(c) shows that the red-detuning magic wavelength for ^{133}Cs $6S_{1/2}$ F = 4 - $6P_{3/2}$ F' = 5 transition is around ~ 935 nm, and our calculation results are in good agreement with previous calculations [5, 6, 13, 14]. Kimble group experimentally implemented 1D standing-wave ODT inside a high-finesse micro-cavity by using ~ 935nm magic wavelength to trap single ^{133}Cs atoms [5]. Figure 2(d) shows that the light shift for all Zeeman sublevels of each hyperfine fold of ^{133}Cs $6P_{3/2}$ states under the condition of the ODT laser wavelength is set to 935nm (magic wavelength for ^{133}Cs $6S_{1/2}$ - $6P_{3/2}$ transition). Zeeman sublevels split by as much as about ± 9% relative to the ground state shift.

4. LIGHT SHIFT OF RUBIDIUM-87 $5S_{1/2}$ AND $5P_{3/2}$ STATES

We also calculated the light shift of ^{87}Rb $5S_{1/2}$ and $5P_{3/2}$ states by considering *n*S states up to 10S, *n*P states up to 10P and *n*D states up to 8D [15]. For ^{87}Rb $5S_{1/2}$ F = 2 - $5P_{3/2}$ F' = 3 transition, we find magic wavelength of ~ 625.3nm and ~789.9nm, but the corresponding polarizability is too small for convenient laser intensity for ODT (in another word the trap depth is too shallow).

Here we try to explore the dichromatic ODT which will have more parameters to be controlled. If we pay motr attentions to the energy level of ^{87}Rb atoms (as shown in Figure 3), ~1.5 μm transitions from $5P_{3/2}$ to 4D states can be used to control the light shift of $5P_{3/2}$ state by using convenient ~ 1.5 μm telecom laser and fiber amplifier. Recently Bouyer group used 1560 nm laser to form ODT to trap ^{87}Rb [16, 17]. Also people calculated dichromatic ODT for Rb atoms [18]. We consider the dichromatic ODT formed by two laser beams with frequency ratio of 2:1 (λ_2=2λ_1). If the ODT laser λ_2 locates at telecom wavelength range (~ 1.5 μm) which is close to the ~1529 nm transitions, it can be employed to efficiently tailor the light shift of $5P_{3/2}$ state and the λ_1 laser can be conveniently achieved via laser frequency doubling technique.

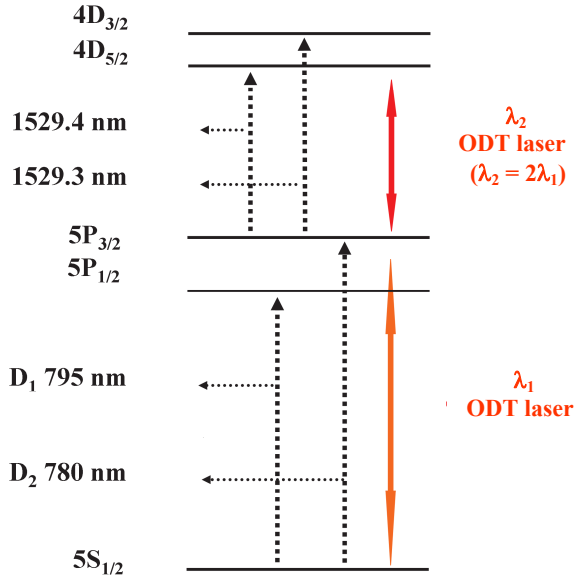

Figure 3. (Color online) The transitions and relevant fine levels of ^{78}Rb atoms which mainly make dominant contributions to the light shift of $5S_{1/2}$ |F = 2> and $5P_{3/2}$ |F' = 3> states when a dichromatic ODT is adopted with an ODT laser beams of λ_1 and λ_2=2λ_1. If the ODT laser λ_2 locates at telecom wavelength range (~ 1.5μm) which is close to the ~1529nm transitions, it can be employed to efficiently tailor the light shift of $5P_{3/2}$ state.

For this linearly-polarized dichromatic ODT, we calculated the light shift of ^{87}Rb $5S_{1/2}$ F = 2 and $5P_{3/2}$ F' = 3 states by considering *n*S states up to 10S, *n*P states up to 10P and *n*D states up to 8D. Again the Einstein *A* coefficients and vacuum wavelengths for the dipole-allowed transitions we considered here come from **[12]**. Calculation results are shown in Figure 4. We find the magic wavelength combinations for $5S_{1/2}$ |F = 2, m = ±2> - $5P_{3/2}$ |F' = 3, m = ±3> transitions at (784.3nm and 1568.6nm) and (806.4nm and 1612.8nm) for both laser beams with the same linear polarization. These dichromatic magic wavelength combinations indeed expand the magic wavelength concept.

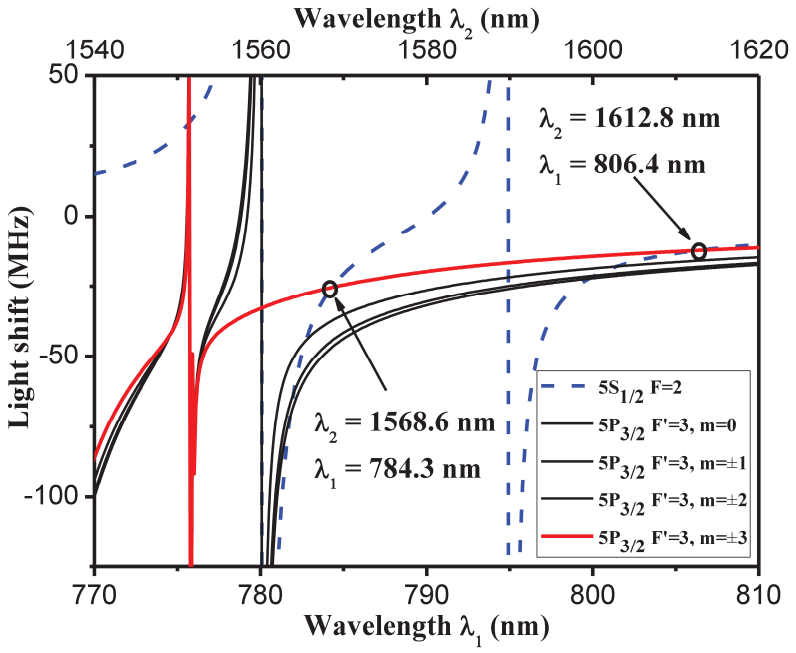

Figure 4. (Color online) The calculated light shift for ^{87}Rb $5S_{1/2}$ F = 2 (dashed blue lines) and $5P_{3/2}$ F' = 3 states (the red solid line is for |F' = 3, m = ±3> states, the other three black solid lines are for |F' = 3, m = 0>, |F' = 3, m = ±1> and |F' = 3, m = ±2> states) when a dichromatic ODT is adopted with same linearly polarized ODT laser beams of λ_1 and $\lambda_2=2\lambda_1$. The optical intensity of both lasers is fixed to 3.6×10^4 W/cm^2 reasonably. Two circles locate the dichromatic magic-wavelength combinations for |F = 2, m = ±2> and |F' = 3, m = ±3> states.

Table 1. Effect of variation in the laser wavelength around dichromatic magic-wavelength combinations upon the light shift of ^{87}Rb $5S_{1/2}$ |F = 2, m = ±2> and $5P_{3/2}$ |F' = 3, m = ±3> states. The data are given under an experimental parameters with an intensity of $I_1 = 2.94\times10^4$ W/cm^2 for 784.3nm laser ($I_1 = 6.17\times10^4$ W/cm^2 for 806.4 nm laser), which forms an ODT potential with a trap depth of ~ 1 mK.

λ_1	$\Delta\lambda_1$	$\lambda_2=2\lambda_1$	U(ground)	U'(excited)	Difference
nm	nm	nm	mK	mK	%
784.2	-0.1	1568.4	-1.03036	-1.00477	2.48
784.3	**0.0**	**1568.6**	**-1.00000**	**-1.00062**	**0.06**
784.4	+0.1	1568.8	-0.96885	-0.99446	2.64
806.3	-0.1	1612.6	-1.00662	-1.00351	0.31
806.4	**0.0**	**1612.8**	**-1.00000**	**-1.00055**	**0.06**
806.5	+0.1	1613.0	-0.99473	-0.99889	0.42

We analyzed the effect of variation in the laser wavelength (but the frequency ratio is kept at 2:1) of the dichromatic laser beams around the magic wavelength combination upon the light shift of the ground and excited states. The results are tabulated in Table 1. The wavelength variations of ± 0.1 nm only make a very little difference in the light shift of the ground and excited states.

We also analyzed the effect of variation in the intensity ratio of the dichromatic laser beams on the light shift of the ground and excited states at magic wavelength combination by varying the intensity ratio ±1% and ±5%. The results are tabulated in Table 2. The small fluctuation in the intensity ratio does not make a substantial effect.

Table 2. Effect of variation in the intensity ratio of 784.3nm and 1568.6nm (806.4nm and 1612.8nm) laser beams at magic-wavelength combination upon the light shift of ^{87}Rb $5S_{1/2}$ |F = 2, m = ±2> and $5P_{3/2}$ |F' = 3, m = ±3> states. The data are given under an experimental parameters with an intensity of $I_1 = 2.94\times10^4$ W/cm^2 for 784.3nm laser ($I_1 = 6.17\times10^4$ W/cm^2 for 806.4 nm laser), which forms an ODT potential with a trap depth of ~ 1 mK.

λ_1	λ_2	I_2/I_1	U (ground)	U'(excited)	Difference
nm	nm		mK	mK	%
784.3	1568.6	0.95	-0.99865	-0.95145	4.73
		0.99	-0.99973	-0.99079	0.89
		1.00	**-1.00000**	**-1.00062**	**0.06**
		1.01	-1.00027	-1.01045	1.02
		1.05	-1.00135	-1.04979	4.84
806.4	1612.8	0.95	-0.99721	-0.94971	4.76
		0.99	-0.99944	-0.99039	0.91
		1.00	**-1.00000**	**-1.00055**	**0.06**
		1.01	-1.00055	-1.01073	1.02
		1.05	-1.00279	-1.05141	4.85

5. LASER SYSTEM FOR MAGIC-WAVELENGTH DICHROMATIC ODT FOR RUBIDIUM-87 ATOMS

For implementing the dichromatic magic wavelength ODT to trap ^{87}Rb atoms, we proposed and experimentally realized a dichromatic laser system based on the quasi-phase-matched (QPM) high-efficiency laser frequency doubling technique with telecom laser and fiber amplifier [19, 20].

In our previous work, 239 mW of 780 nm laser beam was obtained using single-pass frequency doubling from ~ 4.6 W of 1560 nm fundamental-wave laser with a 20-mm-long PPLN bulk crystal (the poled period Λ = 18.8 μm, Deltronics Inc) at ~ 158.2 °C (doubling efficiency of ~ 5.2%) [20]. Here we use a 1568.6 nm extended-cavity diode laser as the seed laser, and employ an Er-doped fiber amplifier (EDFA) to boost laser power to ~ 4W (see Figure 5). Then a PPMgO:LN bulk crystal (size: 1 mm x 3.4 mm x 25 mm, the poled period is Λ = 19.48 μm, HC Photonics Corp) is used for laser frequency doubling from 1568.6nm to 784.3nm. The optimized temperature for phase matching of frequency doubling in the PPMgO:LN bulk crystal is found to be ~ 126.7 °C. The oven housing the PPMgO:LN bulk crystal is stabilized at ±0.01 °C by a temperature controller (not shown in Figure 5).

After frequency doubling, we use dichromatic mirror (DM) to separate the 1568.6 nm fundamental-wave laser beam and the 784.3 nm second-harmonic laser beam, as shown in Figure 5. Then we can conveniently control the power of 1568.6nm laser by using half-wave plate and polarization beam splitter (PBS) cube to reach intensity ratio of 1:1. Finally these dichromatic laser beams are combined by another DM for building the dichromatic magic wavelength ODT for ^{87}Rb atoms. Achromatic doublet lens can be utilized to tightly focus the dichromatic laser beams into a vacuum chamber

where ^{87}Rb atoms are laser cooled and trapped via a magneto-optical trap. Here achromatic doublet lens can make the foci for both of 1568.6 nm and 784.3 nm laser beams at the same position.

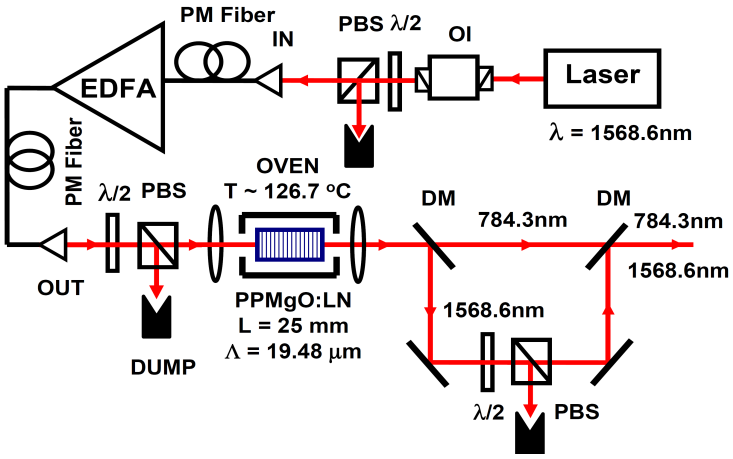

Figure 5. (Color online) Schematic diagram of our laser system based on the quasi-phase-matched (QPM) laser frequency doubling technique with telecom laser and Er-doped fiber amplifier (EDFA) for ^{87}Rb magic-wavelength dichromatic ODT with laser frequency ratio 2:1. Here is an example for the magic wavelength combination of 784.3nm and 1568.6nm with linearly polarized laser beams for ^{87}Rb $5S_{1/2}$ |F = 2, m = +2> - $5P_{3/2}$ |F' = 3, m = +3> (or |F = 2, m = -2> - $5P_{3/2}$ |F' = 3, m = -3>) cycling transition. In principal, the magic wavelength combination of 806.4nm and 1612.8nm with linearly polarized laser beams also can be implemented experimental along the same technique. Key to figure: OI: optical isolator; PBS: polarization beam splitter cube; PM fiber: polarization-maintained optical fiber; EDFA: Er-doped fiber amplifier; DM: dichromatic mirror.

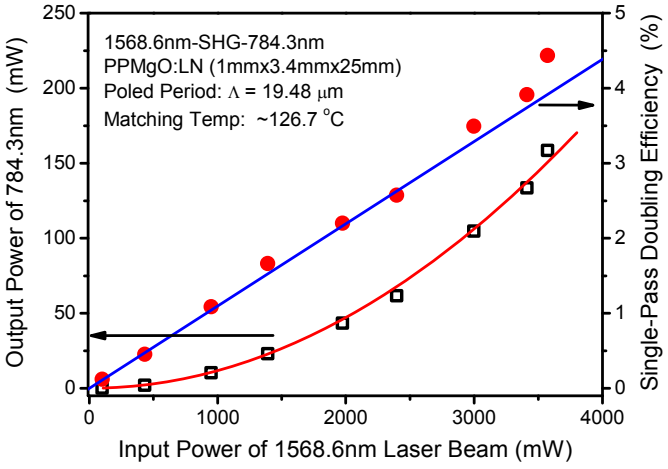

Figure 6. (Color online) This plot shows the 784.3 nm laser's output power (empty black squares) and the doubling efficiency (red dots) from the single-pass QPM frequency doubling via PPMgO:LN bulk crystal versus the 1568.6nm fundamental-wave laser's input power. The solid lines are fitting based on the frequency doubling theoretical model. When the input power of 1568.6nm laser beam is 3.6W, the output power of 784.3nm laser beam is ~ 158mW, which corresponds a maximum single-pass doubling efficiency of 4.4%.

Output power of 784.3 nm second-harmonic laser after single-pass frequency doubling is measured by a laser power meter (Coherent FieldMate + PS-10Q sensor). Measured output power of 784.3 nm second-harmonic laser and the corresponding single-pass doubling efficiency versus the input power of 1568.6 nm fundamental-wave laser beam are

plotted in Figure 6. The 784.3 nm output power of ~ 158 mW is achieved when the 1568.6 nm input power is 3.6 W, and the corresponding single-pass doubling efficiency is 4.4%. From our calculation we know that the trap depth of 784.3 nm/1568.6 nm dichromatic magic wavelength ODT for ^{87}Rb atom can reach 1 ~ 2 mK with a focused waist radius of 10 ~ 15 μm and ~ 100 mW of each component in the dichromatic laser beams. 1 ~ 2 mK of the trap depth is deep enough to trap the laser-cooled atoms.

6. CONCLUSION

We calculated and analyzed the light shift of the ^{133}Cs $6S_{1/2}$ - $6P_{3/2}$ transition for a monochromatic ODT. The monochromatic red-detuning magic wavelength for the ^{133}Cs $6S_{1/2}$ - $6P_{3/2}$ transition at ~ 935 nm is verified, and also a monochromatic blue-detuning magic wavelength at ~ 683 nm is analyzed. Hope we can implement a optical bottle beam ODT with this ~ 683 nm blue-detuning magic wavelength to trap single ^{133}Cs atom to remarkably decrease the photon scattering rate due to ODT laser.

Also we calculated and analyzed the light shift of the ^{87}Rb $5S_{1/2}$ - $5P_{3/2}$ transition for a dichromatic ODT with laser frequency ratio of 2:1. We find that there are dichromatic magic wavelength combinations for $5S_{1/2}$ $|F = 2, m = \pm 2\rangle$ - $5P_{3/2}$ $|F' = 3, m = \pm 3\rangle$ transitions at (784.3 nm and 1568.6 nm) and (806.4 nm and 1612.8 nm) for both laser beams with the same linear polarization. We also proposed and experimentally realized a dichromatic magic-wavelength ODT laser system for ^{87}Rb atoms by employing the high-efficient QPM frequency doubling technique with PPMgO:LN or PPLN bulk crystal and telecom laser as well as EDFA. The dichromatic magic wavelength combination actually expands the magic wavelength concept, and we hope it may find more applications to coherently control the atomic internal state independent of the atomic residual thermal motion and to precisely measure atomic transition frequency.

ACKNOWLEDGEMENT

This research work is supported by the National Natural Science Foundation of China (Grant Nos. 60978017, 61078051 and 11104172), the National Major Scientific Research Program of China (Grant No. 2012CB921601), and the Research Project from Shanxi Scholarship Council of China.

REFERENCES

[1] Chu, S., Bjorkholm, J. E., Ashkin, A. and Cable, A., "Experimental observation of optically trapped atoms," Phys. Rev. Lett. **57**, 314-317 (1986).

[2] Miller, J. D., Cline, R. A. and Heinzen, D. J., "Far-off-resonance optical trapping of atoms," Phys. Rev. A **47**, R4567-R4570 (1993).

[3] For overview of optical dipole trap, see Grimm, R., Weidemuller, M. and Ovchinnikov, Y. B., "Optical dipole traps for neutral atoms," Adv. At. Mol. Opt. Phys. **42**, 95-133 (2000).

[4] Katori, H., Ido, T. and Kuwata-Gonokami, M., "Optimal design of dipole potentials for efficient loading of Sr atoms," J. Phys. Soc. Jpn. **68**(8), 2479-2482 (1999).

[5] McKeever, J., Buck, J. R., Boozer, A. D., Kuzmich, A., Nagerl, H.-C., Stamper-Kurn, D. M. and Kimble, H. J., "State-insensitive cooling and trapping of single atoms in an optical cavity," Phys. Rev. Lett. **90**, 133602 (2003).

[6] Kim, J. Y., Lee, J. S., Han, J. H. and Cho, D., "Optical dipole trap without inhomogeneous ac Stark broadening," J. Korean Phys. Soc. **42**(4), 483-488 (2003).

[7] Takamoto, M., Hong, F.-L., Higashi, R. and Katori, H., "An optical lattice clock," Nature **435**, 321-324 (2005).

[8] Ye, J., Kimble, H. J. and Katori, H., "Quantum state engineering and precision metrology using state insensitive light traps," Science **320**, 1734-1738 (2008).

[9] He, J., Yang, B. D., Zhang, T. C. and Wang, J. M., "Efficient extension of the trapping lifetime of single atom in a microscopic optical tweezer by laser cooling," Phys. Scr. **84**, 025302 (2011).

[10] He, J., Yang, B. D., Cheng, Y. J., Zhang, T. C. and Wang, J. M., "Improvement of the trapping lifetime for a single atom in a far-off-resonance optical dipole trap," Front. Phys. **6**(3), 262-270 (2011).

[11] Darquie, B., Jones, M. P. A., Dingjan, J., Beugnon, J., Bergamini, S., Sortais, Y., Messin, G., Browaeys, A. and Grangier, P., "Controlled single-photon emission from a single trapped two-level atom," Science **309**, 454-456 (2005).

[12] Kurucz, R. L. and Bell, B., "Atomic line data," <http://www.cfa.harvard.edu/amp/ampdata/kurucz23 /sekur.html>.

[13] Zheng, Y. N., Zhou, X. J., Chen, J. B. and Chen, X. Z., "Magic wavelength for cesium transition line $6S_{1/2}$ - $6P_{3/2}$," Chinese Phys. Lett. **23**, 1687-1690 (2006).

[14] Arora, B., Safronova, M. S. and Clark, C. W., "Magic wavelengths for the nP-nS transitions in alkali-metal atoms," Phys. Rev. A **76**, 052509 (2007).

[15] Cheng, Y. J., Qiu, Y., He, J., Zhang, T. C. and Wang, J. M., "Calculation of AC stark shift of $5S_{1/2}$ and $5P_{3/2}$ states of Rb atoms in optical dipole trap," Chinese J. Opt. & Appl. Opt. **3**(2), 119-125 (in Chinese) (2010).

[16] Brantut, J. P., Clement, J. F., Robert de Saint Vincent, M., Varoquaux, G., Nyman, R. A., Aspect, A., Bourdel, T and Bouyer, P., "Light-shift tomography in an optical-dipole trap for neutral atom," Phys. Rev. A **78**, 031401(R) (2008).

[17] Bernon, S., Vanderbruggen, T., Kohlhass, R., Bertoldi, A., Landragin, A. and Bouyer, P., "Heterodyne non-demolition measurements on cold atomic samples: towards the preparation of non-classical states for atom interferometry," New J. Phys. **13**, 065021 (2011).

[18] Arora, B. and Safronova, M. S., "State-insensitive bichromatic optical trapping," Phys. Rev. A **82**, 022509 (2010).

[19] Feng, J. X., Ling, Y. M., Liu, Q., Liu, J. L. and Zhang, K. S., "High-efficiency generation of a continuous-wave single-frequency 780 nm laser by external-cavity frequency doubling," Appl. Opt. **46**, 3593-3596 (2007).

[20] Guo, S. L., Yang, J. F., Yang, B. D., Zhang, T. C. and Wang, J. M., "Frequency doubling of 1560nm diode laser via PPLN and PPKTP crystals and frequency stabilization to rubidium absorption line," Proc. SPIE **7846**, 784619 (2010).